Cellulose (2012) 19:695–703
DOI 10.1007/s10570-012-9683-7

ORIGINAL PAPER

Improvement of mechanical and oxygen barrier properties of cellulose films by controlling drying conditions of regenerated cellulose hydrogels

Quanling Yang · Shuji Fujisawa ·
Tsuguyuki Saito · Akira Isogai

Received: 11 October 2011 / Accepted: 21 February 2012 / Published online: 3 March 2012

Abstract Mechanical, thermal and oxygen barrier properties of regenerated cellulose films prepared from aqueous cellulose/alkali/urea solutions can be markedly improved by controlling the drying conditions of the films. By pre-pressing followed by vacuum drying under compression, the tensile strength, Young's modulus, coefficient of thermal expansion and oxygen permeability of the dried films reached 263 MPa, 7.3 GPa, 10.3 ppm K^{-1} and 0.0007 ml μm m^{-2} day^{-1} kPa^{-1}, respectively. Thus, films produced in this way show the highest performance of regenerated cellulose films with no orientation of cellulose chains reported to date. These improved properties are accompanied by a clear increase in cellulose II crystallinity from 50 to 62% during pre-pressing/press-vacuum drying process. At the same time, the film density increased from 1.45 to 1.57 g cm^{-3}, and the moisture content under equilibrium conditions decreased from 14.1 to 9.8%. Hence, the aqueous alkali/urea solvent system has potential applications in producing new and environmentally friendly cellulose films with high performances through control of the drying conditions.

Electronic supplementary material The online version of this article (doi:10.1007/s10570-012-9683-7) contains supplementary material, which is available to authorized users.

Q. Yang · S. Fujisawa · T. Saito · A. Isogai (✉)
Graduate School of Agricultural and Life Sciences,
The University of Tokyo, 1-1-1 Yayoi, Bunkyo-ku,
Tokyo 113-8657, Japan
e-mail: aisogai@mail.ecc.u-tokyo.ac.jp

Keywords Regenerated cellulose film · Alkali/urea · Drying conditions · Oxygen barrier · Mechanical properties

Introduction

In recent years, there has been a growing demand to develop new bio-based materials with features of renewability, sustainability, biocompatibility, and biodegradability (Ragauskas et al. 2006; Ohlrogge et al. 2009). Cellulose is the most abundant and sustainable biopolymer on earth, with an annual production of 1.5 trillion tons, and it is attracting renewed interest for materials and energy applications (Read and Bacic 2002; Klemm et al. 2005; Kontturi et al. 2006; Heinze and Liebert 2001; Hirota et al. 2010; Rüsch gen. Klaas and Schöne 2009). Regenerated cellulose and nanofibrillated cellulose films have potential applications as bio-based materials with high thermal stability and gas barrier properties because of the highly crystalline and hierarchical network structures of cellulose that arise from abundant and ordered intra- and inter-molecular hydrogen bonds (Hyden 1929; Syverud and Stenius 2009; Nogi et al. 2009; Fukuzumi et al. 2009, 2011; Siró and Plackett 2010; Aulin et al. 2010; Sehaqui et al. 2010; Yang et al. 2011a). Particularly, some regenerated cellulose films (Yang et al. 2011a), nanofibrillated cellulose films (Syverud and Stenius 2009; Fukuzumi et al. 2009, 2011; Aulin et al. 2010) and hemicellulose films

(Zhu Ryberg et al. 2011; Edlund et al. 2010; Hartman et al. 2006) have been studied as bio-based oxygen barrier materials.

In our previous work, transparent and flexible regenerated cellulose films prepared from aqueous alkali (NaOH or LiOH)/urea solutions under suitable regeneration conditions were found to exhibit high oxygen barrier properties that were superior to both conventional cellophane and to those of practical oxygen barrier films such as poly(vinylidene chloride) and poly(vinyl alcohol) (Yang et al. 2011a). Because alkali/urea cellulose solvents are categorized as green systems, which form no hazardous byproducts such as CS_2 or H_2S in the viscose systems (Yang et al. 2009, 2011a, b; Cai et al. 2007, 2008; Liang et al. 2008; Qi et al. 2009), they have potential applications in producing regenerated cellulose films and fibers at the industrial level. The byproducts (mainly Na_2SO_4 and urea) formed in the regeneration bath can be isolated and recycled in the cellulose production system (Qi et al. 2009). Furthermore, properties of regenerated cellulose films prepared from alkali/urea solutions can be widely controlled by controlling the dissolution and regeneration conditions (Yang et al. 2011a). The lowest oxygen permeability of 0.003 ml μm m^{-2} day^{-1} kPa^{-1} was obtained for a cellulose film prepared from a 6 wt% cellulose solution by regeneration with acetone at 0 °C (Yang et al. 2011a). However, because regeneration of cellulose with acetone at 0 °C cannot be used in practical applications, alternative processes to improve mechanical and oxygen barrier properties of cellulose films are required.

Native cellulose fibers such as cotton lint, cotton linters and wood pulps have critical limitations in terms of their variety of formability, whereas systems for dissolution and regeneration of natural celluloses allow us to produce cellulose fibers with various cross-sectional shapes and almost infinite lengths, and cellulose films with uniform thicknesses and large areas. However, regenerated cellulose fibers usually have lower strength than native cellulose fibers because they have lower cellulose II crystallinities than the cellulose I crystallinities of native celluloses (Gindl et al. 2006). The mechanical properties of regenerated cellulose fibers depend on the process parameters (Kong and Eichhorn 2005), and a tensile strength of 1,300 MPa and an elastic modulus of 45 GPa were achieved at the laboratory scale by increasing the degree of orientation of cellulose chains along the fiber axis (Northolt et al. 2001). Cellophanes can be prepared with a tensile strength and an elastic modulus of 125 MPa and 5.4 GPa, respectively, by controlling the degree of orientation of cellulose chains in the films. Regenerated cellulose films prepared from *N*-methylmorpholine-*N*-oxide (NMMO) solutions can have a tensile strength and an elastic modulus of 300 MPa and 8 GPa, respectively (Fink et al. 2001), cellulose films made from solutions in lithium chloride/*N*,*N*-dimethylacetamide can give a tensile strength and an elastic modulus of 396 MPa and 26.4 GPa, respectively (Gindl et al. 2006) and aqueous LiOH/urea cellulose solutions can produce cellulose films with a tensile strength and an elastic modulus of 213 MPa and 11 GPa, respectively (Liu et al. 2009). However, these excellent mechanical properties have been achieved only when measuring in the direction of the highly orientated cellulose chains, while the mechanical properties of the films are significantly poorer when measured in other film directions.

Recently, several drying methods for preparation of regenerated cellulose films (Cai et al. 2010) and nanocellulose films (Fukuzumi et al. 2009; Sehaqui et al. 2010; Nakagaito and Yano 2005), including oven, vacuum, hot-press, and air drying have been studied and the resulting mechanical properties of the films were shown to have vary accordingly. Moreover, nanocellulose films prepared by vacuum drying under compression (press-vacuum drying) resulted in higher tensile strengths and Young's moduli, which were explained by higher in-plane orientations of the nanofibers and also higher film densities caused by drying under constrained conditions of the cellulose nanofibers (Sehaqui et al. 2010). However, the effects of various drying conditions on the detailed properties of regenerated cellulose films have not been reported before now.

In the present work, we report the effects of various drying conditions for regenerated cellulose hydrogel films prepared from aqueous cellulose/alkali/urea solutions on mechanical, thermal and oxygen barrier properties. It was found that these properties were remarkably improved solely by controlling the dying conditions, primarily through control of the crystallinity of cellulose II within the films.

Experimental

Materials

A filter paper pulp (highly purified cotton linters, Advantec Co., Ltd., Japan) was used as the cellulose sample with a viscosity-average molecular weight of 8.6×10^4 g mol^{-1} (Yang et al. 2011a). All reagents and solvents were of laboratory grade (Wako Pure Chemicals, Tokyo, Japan), and used as received.

Preparation of regenerated cellulose hydrogel films

A solvent mixture, LiOH/urea/H_2O with a weight ratio of 4.6:15:80.4 was precooled at −12 °C. A desired amount of cellulose was dispersed in the precooled solvent and the mixture was stirred vigorously at 1,200 rpm for 2 min to form a transparent and viscous solution of a 6 wt% cellulose concentration. The cellulose solution thus obtained (35 ml) was degassed by centrifugation at 10,000 *g* for 10 min, spread on a glass plate, and then immersed in an aqueous solution (~2.5 l) containing 5 wt% H_2SO_4 and 5 wt% Na_2SO_4 at 20 °C for regeneration. The film-like hydrogel of regenerated cellulose thus formed, which had ~1 mm thickness and ~500 cm^2 area, was repeatedly washed with an excess volume of water by soaking.

Drying conditions of regenerated cellulose hydrogel films

Each hydrogel film was placed on a metal plate and the periphery of the hydrogel film was stuck on the plate with several Scotch tape strips to avoid shrinkage of the film during drying. Then, the hydrogel films were dried under the following five conditions: Air drying (Drying-1): drying of the hydrogel film on the metal plate at 20 °C in air for 24 h, in which the upper side of the hydrogel film was exposed to air; vacuum drying (Drying-2): drying of the hydrogel film on the metal plate at various atmospheric pressures in a vacuum oven at 20 °C, in which the upper side of the hydrogel film was exposed to air at a reduced pressure; press-vacuum drying (Drying-3): the hydrogel film was sandwiched between two metal plates and loaded under various compressive pressures controlled with steel weights placed on the upper metal plate in a vacuum oven at 1 kPa and 20 °C for 11 h; pre-pressing and press-vacuum drying (Drying-4): the hydrogel film was sandwiched between two metal plates and loaded at a 1.5 MPa compressive pressure using a press in air at 20 °C for 1 h, followed by the above press-vacuum drying at a compressive pressure of 4 kPa in a vacuum oven at 1 kPa and 20 °C for 11 h; and pre-pressing and press-vacuum-heat drying (Drying-5): the hydrogel films pre-pressed under the above conditions were subsequently dried under press-vacuum conditions at a compressive pressure of 4 kPa in a vacuum oven at 1 kPa and 20–80 °C. All cellulose films were conditioned at 23 °C and 50% relative humidity (RH) for more than 2 days before testing. In the case of measurement of oxygen transmission rates, the cellulose films were further dried in a desiccator containing P_2O_5 at room temperature and 0% RH for at least 3 days.

Analyses

The film thickness was measured with a micrometer and each value was expressed as an average of five measurements. Thicknesses of the cellulose films ranged from 27 to 50 μm, depending on the drying conditions adopted. Statistical errors in thickness of each film were within ±3%. The density of the dried cellulose film was determined from the area, thickness, and dry weight. Oxygen transmission rates of the cellulose films were determined at 23 °C and 0% RH using a Mocon Ox-Tran Model 2/21MH (Modern Controls Inc., USA) under standard conditions (ASTM 3985). Each measurement was continued until the O_2 transmission rate reached a stable value. The oxygen permeability was determined from the oxygen transmission rate and the film thickness, and the standard deviations for each film were within ±5%. Tensile tests were performed using a Shimadzu EZ-TEST instrument equipped with a 500 N load cell. Rectangular strips 2 × 30 mm in size were cut from the cellulose films and tested with a span length of 10 mm at a rate of 1.0 mm min^{-1}. The visible light transmittances of the films were measured from 400 to 800 nm using a Shimadzu UV-1700 UV–Vis spectrophotometer. X-ray diffraction patterns of the films were acquired in reflection mode using a Rigaku RINT 2000 with monochromator-filtered Cu Kα radiation at 40 kV and 40 mA. The crystallinities of the cellulose films were estimated from the areas of diffraction peaks obtained using the Lorentz–Gaussian peak separation method (Rabek 1980). Crystal widths of (1 −1 0) reflections due to cellulose II were calculated from the full widths at half heights of the diffraction peaks by Scherrer's equation (Alexander 1979). Cellulose films were conditioned at 23 °C and 50% RH for 2 days and the moisture contents under these conditions were calculated from the film weights before and after heating at 105 °C for 3 h. Thermal expansivity of the films, which were preheated at 120 °C for 10 min, were determined at 0.03 N load in a nitrogen atmosphere from 28 to 100 °C at 5 °C min^{-1} using a Shimadzu TMA-60 instrument. The films were frozen in liquid nitrogen and immediately snapped and then vacuum-dried. The fracture surfaces (cross-sections) of the films were coated with osmium using a Meiwafosis Neo osmium coater and observed with a Hitachi S4800 field-emission scanning electron microscope at 2 kV.

Results and discussion

Drying conditions of regenerated cellulose hydrogel films

The regenerated cellulose hydrogel films prepared from aqueous cellulose/alkali/urea solutions were dried under five different conditions described in the Experimental section and the fundamental properties of the dried and conditioned films are summarized in Table 1. The drying times listed in Table 1 were fixed based on the results obtained in preliminary experiments, in which the film weight was monitored in terms of drying time under each drying condition. No further loss of weight was observed in each case after the drying time given in Table 1. Vacuum drying (Drying-2) removes water from the hydrogel films in less time than air drying (Drying-1) by forced removal of water under reduced pressure. For the cases of "press-vacuum drying" (Drying-3) and "pre-pressing + press-vacuum drying" (Drying-4) shown in Table 1, longer times were required for the film to reach a constant weight, because water in the hydrogel film was removed only from the small area at the edge of the film, which was sandwiched between two metal plates, even during vacuum drying.

Properties of cellulose films

Thicknesses of the films changed according to the drying conditions and the film densities correspondingly varied from 1.44 to 1.57 g cm^{-3}. X-ray diffraction patterns of the films are presented in Fig. 1, showing that all the films had the same cellulose II crystal structures but different crystallinities. The diffraction intensities clearly increased with the film density and thus the crystallinity of cellulose II as well as the film density is controllable by controlling the drying conditions. In particular, because the diffraction intensity of the (1 −1 0) peak significantly increased with film density, the drying conditions are likely to control the regularity between hydrophilic interactions between cellulose chains of cellulose II, maintaining a similar hydrophobic chain stacking regularity (Hori and Wada 2006).

Drying-4 resulted in the highest film density and the highest crystallinity of cellulose II (Table 1). Probably, highly regular intra- and inter-molecular hydrogen

Table 1 Characteristics of cellulose films prepared from regenerated cellulose hydrogels under various drying conditions

Drying conditions	Drying temp. (°C)	Drying time (h)	Film density (g cm^{-3})	Crystal width[a] (nm)	Crystallinity (%)	Moisture content (%)	CTE[b] (ppm k^{-1})
Drying-1[c]	20	24	1.45 ± 0.01	3.47	50	14.1	15.5
Drying-2[d]	20	3	1.51 ± 0.03	3.56	53	12.5	14.0
Drying-3[e]	20	11	1.55 ± 0.01	3.68	58	11.4	11.6
Drying-4[f]	20	11	1.57 ± 0.02	3.78	62	9.8	10.3
Drying-5[g]	80	6	1.44 ± 0.02	3.40	47	15.8	16.1

[a] Crystal width of the (1 −1 0) reflection peak due to cellulose II

[b] CTE: Coefficient of thermal expansion

[c] Air drying

[d] Vacuum drying at air pressure of 1 kPa

[e] Press-vacuum drying at compressive pressure of 4 kPa

[f] Pre-pressing and press-vacuum drying

[g] Pre-pressing and press-vacuum-heat drying

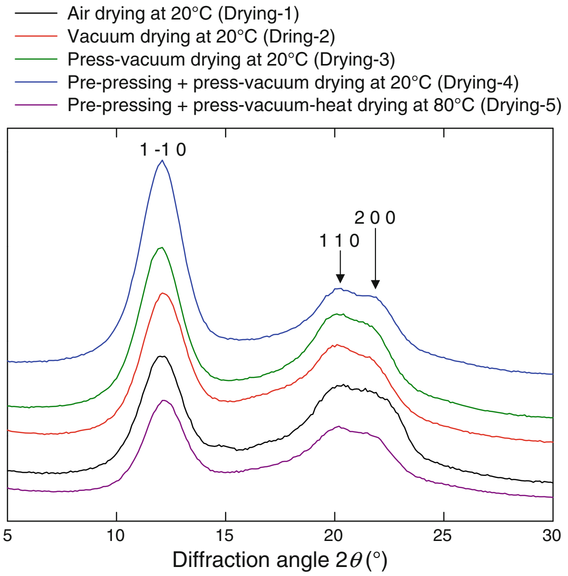

Fig. 1 X-ray diffraction patterns of cellulose films prepared from regenerated cellulose hydrogel films under different drying conditions. See Table 1 and the “Experimental” section for details of the drying conditions

bonds of cellulose chains are formed during these two water-removal processes, in which water molecules within the hydrogel films are somewhat forcibly removed by the pre-pressing, pressing and vacuum drying treatments. On the other hand, rapid removal of water from the hydrogel films by Drying-5 at 80 °C led to a lower film density and lower crystallinity, indicating that high mobility of water molecules in the hydrogel films at high temperatures may have resulted in less regularity in terms of intra- and intermolecular hydrogen bond formation in the cellulose films.

Moreover, as the cellulose II crystallinity of the cellulose films was increased, correspondingly both the moisture content at 23 °C and 50% relative humidity (RH) and the coefficient of thermal expansion (CTE) decreased (Table 1). A CTE value of 10 ppm K^{-1} was sufficiently low under dry conditions and close to that of glass (~9 ppm K^{-1}) (Fukuzumi et al. 2009) or iron (~11.8 ppm K^{-1}) (Nishino et al. 2004). Moreover, the CTE values of the cellulose films in Table 1 are much lower than those of most plastics (>50 ppm K^{-1}) (Nogi et al. 2009), because of the high crystallinity of the cellulose films. As shown in Figure S1 in the supplementary material file, linear correlations were obtained between the film density and either the crystallinity, crystal width, moisture content or CTE of the films. In addition, good correlations between the density or crystallinity of the films and either tensile strength or Young’s modulus were obtained, as shown in Figure S2 in the supplementary material file. Thus, the forced removal of water from the cellulose hydrogel films by vacuum drying effectively improves the mechanical properties of the films by increasing the crystallinity of cellulose II (see X-ray diffraction patterns of the samples prepared by Drying-1 and Drying-2 in Fig. 1).

Effects of drying conditions on mechanical and optical properties of regenerated cellulose films

Figure 2 shows the effects of compression of cellulose hydrogel films during press-vacuum drying (Drying-3) at 20 °C and 1 kPa on tensile strength and Young’s modulus of the cellulose films. These parameters increased from 164 to 249 MPa and from 5.2 to 6.8 GPa, respectively, when the compressive pressure was increased from 0 to 4 kPa. Thus, compression applied to the cellulose hydrogel films during vacuum drying is quite effective in increasing the tensile strength and Young’s modulus of the cellulose films as well as the crystallinity of cellulose II (see X-ray diffraction patterns of the samples prepared by Drying-2 and Drying-3 in Fig. 1). It was reported that mechanical properties of nanocellulose films are improved by vacuum drying of hydrogel films under constrained conditions (Sehaqui et al. 2010) which is

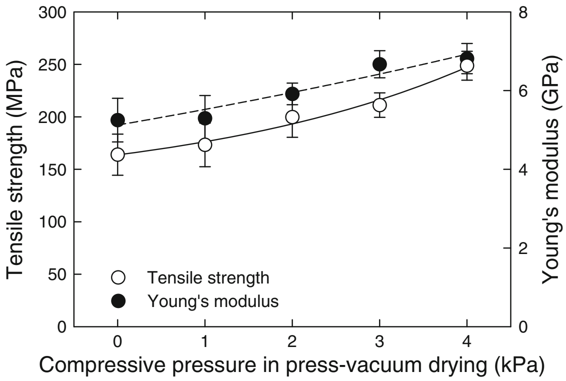

Fig. 2 Effects of compression of the regenerated cellulose hydrogel films during vacuum drying at 1 kPa and 20 °C for 11 h (Drying-3) on tensile strength and Young’s modulus of dried cellulose films

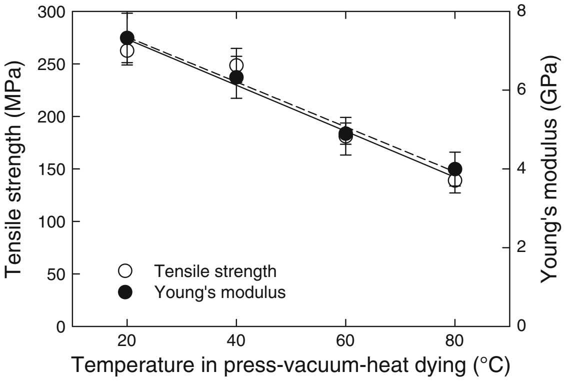

Fig. 3 Effects of temperature during press-vacuum drying (Drying-5) of the pre-pressed cellulose hydrogel films on tensile strength and Young's modulus of dried cellulose films

consistent with the results of Drying-3 used in this study.

The effects of pre-pressing the cellulose hydrogel films at 1.5 MPa at 20 °C for 1 h using a press machine on the tensile strength and Young's modulus of the cellulose films are presented in Figure S3 in the supplementary material file. The tensile strength and Young's modulus of the films were further increased by the pre-pressing.

Figure 3 shows the effects of temperature during Drying-5 of the cellulose hydrogel films on tensile strength and Young's modulus. All films were pre-pressed at 1.5 MPa for 1 h before Drying-5. Tensile strength and Young's modulus decreased from 263 to 139 MPa and from 7.3 to 4.0 GPa, respectively, as the temperature was increased from 20 to 80 °C, i.e. relative decreases of 47 and 45%, respectively, with increasing temperature. The drying time can be reduced by Drying-5 at higher temperatures, because water is removed from the cellulose hydrogel films more effectively than at low temperatures. However, the rapid removal of water molecules from the cellulose hydrogel films by heating has a negative impact on the mechanical properties and reduces the increase in crystallinity (see the X-ray diffraction patters of the samples prepared by Drying-4 and Drying-5 in Fig. 1).

The stress–strain curves of the cellulose films prepared under different drying conditions in Table 1 are shown in Figure S4 in the supplementary material file. Tensile strengths and Young's moduli of the films varied, depending on the drying conditions, but no obvious differences in elongations at break, i.e. 13–14%, were observed amongst the cellulose films. It is probable that the tensile strengths and Young's moduli are strongly influenced by crystallinity or density of the films, whereas elongation is primarily influenced by the properties of disordered regions in the cellulose films, which may be similar between the cellulose films dried under different conditions.

Figure S5 in the supplementary material file shows the visible light transmittances of the cellulose films with a normalized thickness of 40 µm prepared under different drying conditions. The light transmittances of all the films at 600 nm were quite similar and sufficiently high, ranging from 88 to 90%, which are suitable for transparent packaging films and flat display panels. Thus, the light transmittances are not significantly influenced by film density or the crystallinity of the films, which depend on the drying conditions of the cellulose hydrogel films.

Effect of drying conditions on oxygen permeability of regenerated cellulose films

Figure 4 shows the effects of air pressure during vacuum drying (Drying-2) of the regenerated cellulose hydrogel films at 20 °C on the oxygen permeability of the obtained cellulose films, normalized by the film thicknesses. The oxygen permeability markedly decreased from 0.0124 to 0.0078 ml µm m^{-2} day^{-1} kPa^{-1} (37% to the original value) as the air pressure of vacuum drying was reduced from atmospheric pressure to 1 kPa. 1 kPa was the lowest air pressure possible using the laboratory vacuum oven in this

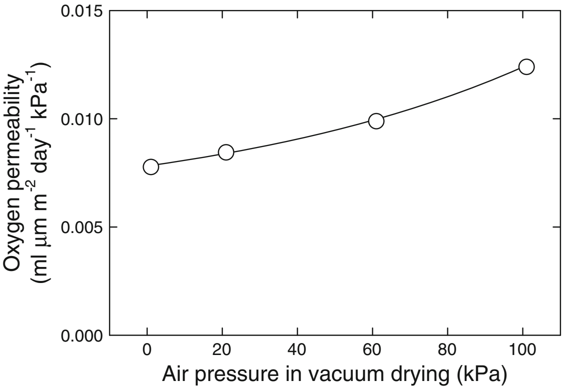

Fig. 4 Effect of air pressure during vacuum drying (Driyng-2) of regenerated cellulose hydrogel films at 20 °C on oxygen permeability of dried cellulose films

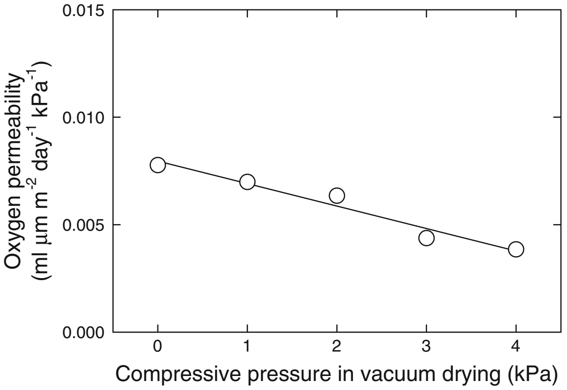

Fig. 5 Effect of compression of regenerated cellulose hydrogel films during vacuum drying at 1 kPa and 20 °C for 11 h (Drying-3) on oxygen permeability of dried cellulose films

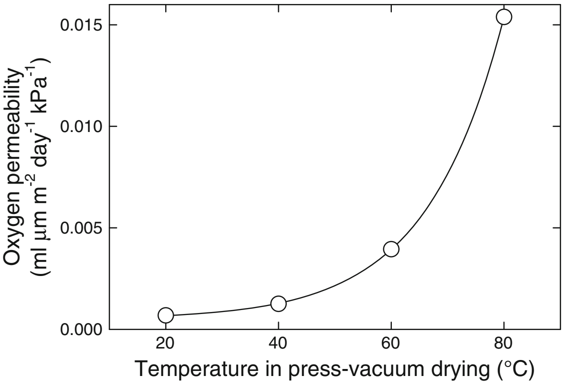

Fig. 6 Effect of temperature during press-vacuum drying (Drying-5) of the pre-pressed cellulose hydrogel films on oxygen permeability of dried cellulose films

work. The increase in cellulose II crystallinity and the dense structures of the film by vacuum drying at low pressures may have resulted in the low oxygen permeability of the cellulose film.

The effects of compression of the regenerated cellulose hydrogel films during press-vacuum drying at 1 kPa and 20 °C (Drying-3) on oxygen permeability are shown in Fig. 5. The oxygen permeability was further reduced from 0.0078 to 0.0038 ml µm m^{-2} day^{-1} kPa^{-1} (51% to the original value) as the compressive pressure was increased from 0 to 4 kPa in this case. This result exhibits that vacuum drying with compression pressure is quite effective in improving the oxygen barrier properties of the regenerated cellulose films.

In addition, we applied pre-pressing of the cellulose hydrogel films at 1.5 MPa for 1 h using a press before the films were subjected to press-vacuum drying at 1 kPa and 20 °C (Drying-4). The oxygen permeability of the films markedly decreased from 0.0038 (by Drying-3) to 0.0007 ml µm m^{-2} day^{-1} kPa^{-1} (a reduction of 82% of the original value) by press-vacuum drying combined with the pre-pressing treatment (Drying-4). This oxygen permeability value is close to those of nanofibrillated cellulose films (Aulin et al. 2010, Fukuzumi et al. 2011), and extremely low in comparison with those of other bio-based or petroleum-based polymer films. For example, films made of microcrystalline wax, arabinoxylan, collagen, chitosan–glycerol (4:1 by weight), high-density poly(ethylene), poly(ethylene terephthalate), nylon-6, poly(vinylidene chloride), poly(vinyl alcohol) and ethylene vinyl alcohol have oxygen permeabilities of 1,540, 2, 1.2, 0.01–0.04, 500, 8, 6, 0.4, 0.04 and 0.01–0.1 ml µm m^{-2} day^{-1} kPa^{-1} at 0% RH, respectively (Ebina and Mizukami 2007; Aulin et al. 2010).

Figure 6 shows the effect of drying temperature during Drying-5 on oxygen permeability of the cellulose films. The drying times were set to 11, 10, 8 and 6 h at heating temperatures of 20, 40, 60 and 80 °C, respectively, because higher the temperatures resulted in shorter drying times. The oxygen permeability of the films increased from 0.0007 to 0.0154 ml µm m^{-2} day^{-1} kPa^{-1}, as the drying temperature was increased from 20 to 80 °C. Thus, the rapid removal of water molecules from the cellulose hydrogel films by heating at high temperatures had a negative impact on oxygen permeability and the increase in crystallinity of the films (see the X-ray diffraction patterns of the samples prepared by Drying-4 and Drying-5 in Fig. 1). Drying-5 at high temperatures causes lower film density, lower crystallinity and results in higher oxygen permeability of the films, indicating that high mobility of water molecules within the hydrogel films at high temperatures during the drying process may bring about less regularity in terms of intra- and inter-molecular hydrogen bond formation in the cellulose films.

SEM images of cross sections of the cellulose films prepared by Drying-1 and Drying-4 of the cellulose hydrogel films are shown in Fig. 7. The film prepared by Drying-4 clearly had denser structures compared with the film prepared by air drying. Thus, pre-pressing and subsequent press-vacuum drying is

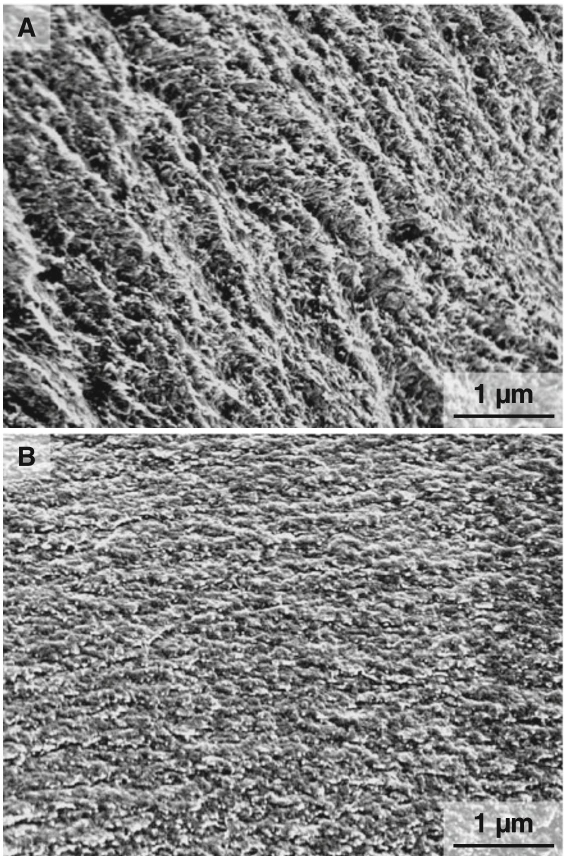

Fig. 7 SEM images of cross-sections of cellulose films prepared by Drying-1 (A) and Drying-4 (B)

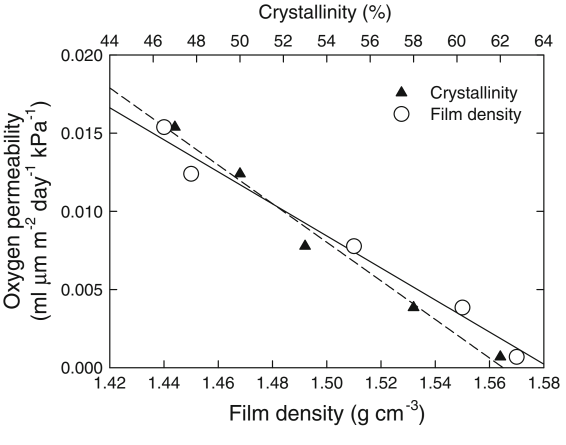

Fig. 8 Relationships between either film density or crystallinity and oxygen permeability of regenerated cellulose films

effective in the formation of cellulose films with a denser structure or a less porous structure, as well as a higher cellulose II crystallinity which leads to higher oxygen barrier properties, improved mechanical properties and lower coefficients of thermal expansion. The correlations between either the density or crystallinity of the cellulose films prepared under the different drying conditions and the oxygen permeability of the films at 0% RH are presented in Fig. 8, which shows clearly linear relationships between these three factors.

Conclusion

The mechanical, thermal and oxygen barrier properties of cellulose films prepared by regeneration from aqueous cellulose/alkali/urea solutions can be significantly improved by controlling the drying conditions. Cellulose films prepared by Drying-4 had the highest film density (1.57 g cm^{-3}), crystallinity (62%), tensile strength (263 MPa) and Young's modulus (7.3 GPa), and the lowest moisture content (9.8%), coefficient of thermal expansion (10.3 ppm K^{-1}) and oxygen permeability (0.0007 ml µm m^{-2} day^{-1} kPa^{-1}). These mechanical, thermal and oxygen barrier properties are clearly superior to those of regenerated cellulose films without orientation of cellulose chains, prepared using the conventional viscose, NMMO and other cellulose solvent systems. Thus, aqueous alkali/urea solvent systems for cellulose have potential applications in producing new and environmentally friendly cellulose films with high performances by controlling the drying conditions of regenerated cellulose hydrogel films. However, because long drying times were required in laboratory-scale experiments, more efficient drying processes and systems should be developed for practical production of regenerated cellulose films.

Acknowledgments This study was partially supported by the Japan Society for the Promotion of Science (JSPS), Grant-in-Aid for Scientific Research S (grant number 21228007), and by the China Scholarship Council (CSC) for QY.

References

Alexander LE (1979) X-ray diffraction methods in polymer science. Robert E. Kreiger Publishing Co., Humington, pp 423–424

Aulin C, Gällstedt M, Lindström T (2010) Oxygen and oil barrier properties of microfibrillated cellulose films and coatings. Cellulose 17:559–574

Cai J, Zhang L, Zhou J, Qi H, Chen H, Kondo T, Chen X, Chu B (2007) Multifilament fibers based on dissolution of cellulose in NaOH/urea aqueous solution: structure and properties. Adv Mater 19:821–825

Cai J, Kimura S, Wada M, Kuga S, Zhang L (2008) Cellulose aerogels from aqueous alkali hydroxide–urea solution. ChemSusChem 1:149–154

Cai J, Wang Q, Zhang L (2010) Prepare of a kind of high strength and optically transparent cellulose material. China Patent ZL20100235233.1

Ebina T, Mizukami F (2007) Flexible transparent clay films with heat-resistant and high gas-barrier properties. Adv Mater 19:2450–2453

Edlund U, Zhu Ryberg YZ, Albertsson AC (2010) Barrier films from renewable forestry waste. Biomacromolecules 11:2532–2538

Fink HP, Weigel P, Purz HJ, Ganster J (2001) Structure formation of regenerated cellulose materials from NMMO-solutions. Prog Polym Sci 26:1473–1524

Fukuzumi H, Saito T, Iwata T, Kumamoto Y, Isogai A (2009) Transparent and high gas barrier films of cellulose nanofibers prepared by TEMPO-mediated oxidation. Biomacromolecules 10:162–165

Fukuzumi H, Saito T, Iwamoto S, Kumamoto Y, Ohdaira T, Suzuki R, Isogai A (2011) Pore size determination of TEMPO-oxidized cellulose nanofibril films by positron annihilation lifetime spectroscopy. Biomacromolecules 12:4057–4062

Gindl W, Martinschitz KJ, Boesecke P, Keckes J (2006) Changes in the molecular orientation and tensile properties of uniaxially drawn cellulose films. Biomacromolecules 7:3146–3150

Hartman J, Albertsson AC, Sjöberg J (2006) Surface- and bulk-modified galactoglucomannan hemicellulose films and film laminates for versatile oxygen barriers. Biomacromolecules 7:1983–1989

Heinze T, Liebert T (2001) Unconventional methods in cellulose functionalization. Prog Polym Sci 26:1689–1762

Hirota M, Furihata K, Saito T, Kawada T, Isogai A (2010) Glucose/glucuronic acid alternating co-polysaccharides prepared from TEMPO-oxidized native celluloses by surface peeling. Angew Chem Int Ed 49:7670–7672

Hori R, Wada M (2006) The thermal expansion of cellulose II and III_{II} crystals. Cellulose 13:281–290

Hyden WL (1929) Manufacture and properties of regenerated cellulose films. Ind Eng Chem 21:405–410

Klemm D, Heublein B, Fink HP, Bohn A (2005) Cellulose: fascinating biopolymer and sustainable raw material. Angew Chem Int Ed 44:3358–3393

Kong K, Eichhorn SJ (2005) Crystalline and amorphous deformation of process-controlled cellulose-II fibres. Polymer 46:6380–6390

Kontturi E, Tammelin T, Österberg M (2006) Cellulose—model films and the fundamental approach. Chem Soc Rev 35:1287–1304

Liang S, Wu J, Tian H, Zhang L, Xu J (2008) High-strength cellulose/poly(ethylene glycol) gels. ChemSusChem 1:558–563

Liu S, Zhang L, Sun Y, Lin Y, Zhang X, Nishiyama Y (2009) Supramolecular structure and properties of high strength regenerated cellulose films. Macromol Biosci 9:29–35

Nakagaito AN, Yano H (2005) Novel high-strength biocomposites based on microfibrillated cellulose having nano-order-unit web-like network structure. Appl Phys A-Mater Sci Process 80:155–159

Nishino T, Matsuda I, Hirao K (2004) All-cellulose composite. Macromolecules 37:7683–7687

Nogi M, Iwamoto S, Nakagaito A, Yano H (2009) Optically transparent nanofiber paper. Adv Mater 21:1595–1598

Northolt MG, Boerstoel H, Maatman H, Huisman R, Veurink J, Elzerman H (2001) The structure and properties of cellulose fibres spun from an anisotropic phosphoric acid solution. Polymer 42:8249–8264

Ohlrogge J, Allen D, Berguson B, DellaPenna D, Shachar-Hill Y, Stymne S (2009) Driving on biomass. Science 324:1019–1020

Qi H, Chang C, Zhang L (2009) Properties and applications of biodegradable transparent and photoluminescent cellulose films prepared via a green process. Green Chem 11:177–184

Rabek J (1980) Experimental methods in polymer chemistry. Wiley, Chichester

Ragauskas AJ, Williams CK, Davison BH, Britovsek G, Cairney J, Eckert CA, Rederick WJ, Hallett JP, Leak DJ, Liotta CL, Mielenz JR, Murphy R, Templer R, Tschaplinski T (2006) The path forward for biofuels and biomaterials. Science 311:484–489

Read SM, Bacic T (2002) Prime time for cellulose. Science 295:59–60

Rüsch gen. Klaas M, Schöne H (2009) Direct, high-yield conversions of cellulose into biofuel and platform chemicals-on the way to a sustainable biobased economy. ChemSusChem 2:127–128

Sehaqui H, Liu A, Zhou Q, Berglund LA (2010) Fast preparation procedure for large, flat cellulose and cellulose/inorganic nanopaper structures. Biomacromolecules 11:2195–2198

Siró I, Plackett D (2010) Microfibrillated cellulose and new nanocomposite materials: a review. Cellulose 17:459–494

Syverud K, Stenius P (2009) Strength and barrier properties of MFC films. Cellulose 16:75–85

Yang Q, Lue A, Qi H, Sun Y, Zhang X, Zhang L (2009) Properties and bioapplications of blended cellulose and corn protein films. Macromol Biosci 9:849–856

Yang Q, Fukuzumi H, Saito T, Isogai A, Zhang L (2011a) Transparent cellulose films with high gas barrier properties fabricated from aqueous alkali/urea solutions. Biomacromolecules 12:2766–2771

Yang Q, Qin X, Zhang L (2011b) Properties of cellulose films prepared from NaOH/urea/zincate aqueous solution at low temperature. Cellulose 18:681–688

Zhu Ryberg YZ, Edlund U, Albertsson AC (2011) Conceptual approach to renewable barrier film design based on wood hydrolysate. Biomacromolecules 12:1355–1362